Adapter Protein for Site-Specific Conjugation of Payloads for Targeted Drug Delivery

Marina V. Backer,*,† Timur I. Gaynutdinov,† Vimal Patel,† Brian T. Jehning,† Eugene Myshkin,‡ and Joseph M. Backer†

Rammelkamp Center for Research, Case Western Reserve University School of Medicine, Cleveland, Ohio 44109, and SibTech, Inc., Newington, Connecticut 06111. Received March 3, 2004; Revised Manuscript Received July 21, 2004

High-affinity interactions of two fragments of human RNase I (1−15-aa Hu-tag and 21−125-aa HuS adapter protein) can be used for assembly of targeting drug delivery complexes. In this approach, a targeting protein is expressed as a fusion protein with a 15-aa Hu-tag, while HuS is conjugated to a drug (or a drug carrier) creating a "payload" module, which is then bound noncovalently to the Hu-tag of the targeting protein. Although this approach eliminates chemical modifications of targeting proteins, the payload modules are still constructed by random cross-linking of drugs or drug carriers to an adapter protein that might lead to functional heterogeneity of the complexes. To avoid this problem, we engineered an adapter protein HuS(N88C) with an unpaired cysteine in position 88 that can be directly modified without interference with activity of assembled targeting complexes. HuS(N88C) binds Hu-tagged annexin V with K_D of 50 ± 6 nM, which is comparable to that of wild-type HuS. To demonstrate the utility of HuS(N88C) for developing uniform payload modules, we constructed a HuS(N88C)−lipid conjugate and inserted it into preformed liposomes loaded with a fluorescent dye. Targeting proteins, Hu-tagged vascular endothelial growth factor or Hu-tagged annexin V, were docked to liposomes decorated with HuS, and the assembled complexes delivered liposomes selectively to target cells.

INTRODUCTION

Efficient technology for loading drugs or drug carriers onto targeting proteins is necessary for targeted drug delivery (*1*). Currently, loading is largely based on random chemical conjugation of a cargo, such as drugs, drug carriers, or adapters for drug carriers, directly to targeting proteins. Chemical modifications of targeting proteins often damage their ability to bind to cellular targets, require expensive custom development, and yield heterogeneous preparations. To solve these problems, we have recently proposed to link a cargo to a standardized adapter protein that binds noncovalently to a docking tag engineered into a targeting protein (*2*). Our current adapter/docking tag pair is based on interactions between two fragments of human RNase I (*3*). As an adapter protein, we are using a 21−127-amino acid (aa) fragment of human RNase I, named HuS, while its N-terminal 1−15-aa fragment fused to a targeting protein serves as a docking tag, named Hu-tag. In the first application of this approach in vivo, we imaged a small mouse tumor using assembled complexes of Tc^{99m}-radiolabeled HuS and Hu-tagged vascular endothelial growth factor (*4*).

Although this approach eliminates chemical modifications of targeting proteins, assembled complexes are still structurally (and, potentially, functionally) heterogeneous because an adapter protein is still loaded via random cross-linking. Furthermore, random chemical modifications of adapter protein, particularly with large cargos such as liposomes or nanoparticles, decrease a proportion of molecules retaining full tag-binding activity. To solve these problems, we engineered an adapter protein with an unpaired cysteine in position 88, HuS(N88C), that can be directly modified without interference with activity of assembled targeting complexes. In this work, a PEGylated lipid was cross-linked to C88 in HuS(N88C), and the resulting conjugate was used to decorate liposomes (Figure 1). Hu-tagged vascular endothelial growth factor, or Hu-tagged annexin V, was docked to HuS−liposomes, and assembled complexes delivered liposomes selectively to target cells.

MATERIALS AND METHODS

Construction and Purification of Chimeric BH−RNase Mutants. Construction of chimeric $^{1-29}$B/$^{30-127}$H-RNase (BH-RNase) consisting of a 1−29 aa fragment of bovine RNase A and a 30−127 aa fragment of human RNase I has been described recently (*5*). The N88C and G68C amino acid substitutions were introduced separately in the pET29/$^{1-29}$B/$^{30-127}$H-RNase plasmid DNA by site-directed mutagenesis (Gene-Tailor site-directed mutagenesis kit, Invitrogen, Carlsbad, CA). The following primers were used for mutagenesis: 5′-TC ACT GAC TGC CGT CTT ACT TGC GGA TCC CGT T (sense, mutation underlined) and 5′-AGT AAG ACG GCA GTC AGT GAT ATG CAT AGA A (antisense) for the N88C mutation and 5′-AG AAG GTT ACC TGC AAA AAT TGC CAG GGT AAC TG (sense, mutation underlined) and 5′-ATT TTT GCA GGT AAC CTT CTC TTG GAA GCA A (antisense) for the G68C mutation. Both mutations were confirmed by sequencing. BH-RNase(G68C) and BH-RNase(N88C) were expressed in BL21(DE3) *Escherichia coli* (Novagen,

* To whom correspondence should be addressed. Mailing address: SibTech, Inc., 705 North Mountain Road, Newington, CT 06111. Phone: (860) 953-1753. Fax: (860) 953-1317. E-mail: mbacker@sibtech.com.

† SibTech, Inc.

‡ Case Western Reserve University School of Medicine.

10.1021/bc0499477 CCC: $27.50
Published on Web 00/00/0000 **PAGE EST: 8.2**

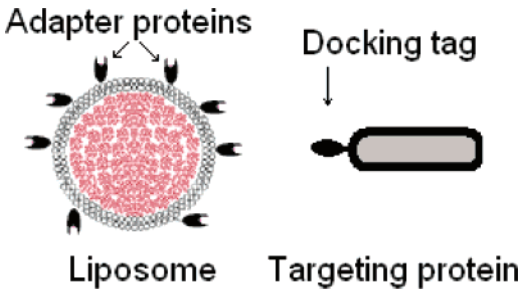

Figure 1. Assembly of targeting complexes for drug delivery.

Madison, WI), refolded from inclusion bodies, and purified by ion-exchange chromatography on HiTrap SP Sepharose Fast Flow (1-mL prepacked columns, Amersham Biosciences, Piscataway, NJ) as described for BH-RNase (*5*). Free SH-groups in proteins were detected by reaction with *N*-(1-pyrene)-maleimide (Molecular Probes, Eugene, OR) as described (*6*). Briefly, *N*-(1-pyrene)-maleimide dissolved in DMSO was added to an assayed protein at the molar ratio of 10:1 and incubated for 1 h at RT (conditions yielding no modification in wild-type BH-RNase). The reaction mixture was analyzed by reverse-phase high-performance liquid chromatography (RP HPLC) on a C4 Alltech MACROSPHERE 300 5 μm column (150 mm × 4.6 mm) with elution at 0.75 mL/min with 0.1% TFA (v/v) and a linear gradient of acetonitrile (5−50% over 15 min) with detection at 216 and 340 nm.

Purification of HuS Mutants. To release 21−127-aa HuS(N88C) and HuS(G68C) proteins, the corresponding BH-RNase mutants were digested with subtilisin (Sigma, St. Louis, MD) at the protein to protease w/w ratio of 50:1. After a 1-hr digestion at 4 °C, the reactions were stopped by ice-cold TFA (a final concentration of 1%), and HuS mutants were purified by affinity chromatography on a column carrying CA-extended Hu-peptide (**CA**-KESRAKKFQRQHMDS synthesized by Genemed Synthesis, Inc., South San Francisco, CA) as described (*5*). Bound HuS mutants were eluted with 0.1 M citric acid, neutralized with 1 M Na_2HPO_4, and stored at −70 °C in small aliquots. Purified proteins were analyzed by RP HPLC on C18 Waters Nova-Pack 5 μm column (150 mm × 3.9 mm) with elution at 0.75 mL/min with 0.1% TFA (v/v) and a linear gradient of acetonitrile (5−50% over 20 min). The concentrations of HuS mutants were calculated using 216-nm integral absorption in HPLC profiles with bovine S-protein (Sigma) serving as a standard.

To obtain HuS(N88C) with a free C88 SH-group, BH-RNase(N88C) was incubated at 4 °C for 16 h in the presence of 1.5-fold molar access of DTT and 0.5 M NDSB-221 (Novagen) followed by subtilisin digestion and affinity purification as described above. To assign the free SH group, deprotected HuS(N88C) was labeled with *N*-(1-pyrene)-maleimide (Molecular Probes) and digested with endopeptidase Arg-C (Roche) according to the manufacturer's instructions. The digest was separated on RP HPLC C4 column, and a single peak containing 87% of incorporated pyrene was collected and analyzed by electrospray mass spectrometry at Yale Cancer Center Mass Spectrometry Resources and the W. M. Keck Foundation Biotechnology Resource Laboratory (New Haven, CT).

Modification of HuS(N88C) with Poly(ethylene glycol)−α-Distearoyl Phosphatidylethanolamine−ω-maleimide (mPEG−DSPE−maleimide). Twenty milligrams of BH-RNase(N88C) was incubated at 4 °C for 16 h in the presence of 1.5-fold molar access of DTT and 0.5 M NDSB-221 (Novagen) and then digested with subtilisin (w/w ratio of 50:1) for 2 h at 4 °C. Subtilisin digestion was stopped by ice-cold TFA (a final concentration of 1%), and the reaction mixture was loaded onto a HiTrap SP Sepharose column equilibrated with 20 mM NaOAc, 0.2 M NaCl, and 0.5% TFA. Subtilisin was completely removed from the column with 0.2 M NaCl, 20 mM NaOAc, while digested BH-RNase was eluted with 0.6 M NaCl, 20 mM NaOAc, pH 6.5. Eluted protein was incubated with mPEG−DSPE−maleimide (FW 3400, Shearwater Polymers, Huntsville, AL) at the molar protein-to-lipid ratio of 1:10 for 2 h at RT. The reaction mixture was then passed through a Hu-peptide affinity column. The mixture of HuS(N88C)−DSPE and unmodified HuS(N88C) bound to the column was eluted with 0.1 M citric acid, neutralized with 1 M Na_2HPO_4, and analyzed by RP HPLC on a Vydac Diphenyl (219TP5415) column (250 mm × 4.6 mm) with elution at 0.75 mL/min with 50 mM thriethylamine phosphate, pH 2.8, 20% 2-propanol with a linear gradient of acetonitrile (0−70% over 30 min). The eluted mixture was stored in liquid nitrogen in small aliquots.

Preparation of HuS−Liposomes. Liposomes containing 1,2-dioleoyl-*sn*-glycero-3-phosphocholine (DOPC, FW 786.15, Avanti, Alabaster, AL) and cholesterol (FW 386.7, Sigma) at the ratio of 65:35 (%) were prepared as described (2). A fluorescent dye, 8-hydroxypyrene-1,3,6-trisulfonic acid, trisodium salt (HPTS, Sigma), was added to the lipid hydration mixture at a concentration of 35 mM. Free HPTS was separated from liposomes by chromatography on Sepharose CL-4B (Sigma). The HPTS-loaded liposomes were incubated with 2.5 μM HuS-(N88C)−DSPE at 37 °C for 16 h in a volume of 1 mL, and then passed again through Sepharose CL-4B column. The efficiency of HuS(N88C)−DSPE insertion was analyzed by RP HPLC on a Vydac Diphenyl (219TP5415) column (250 mm × 4.6 mm) with elution at 0.75 mL/min with 50 mM thriethylamine phosphate, pH 2.8, and 20% tetrahydrofuran with a linear gradient of acetonitrile (0−70% over 25 min). In four independent preparations, concentration of liposomal HuS(N88C) determined by RP HPLC was 2 ± 0.4 μM. The HPTS content determined fluorometrically at λ_{ex} = 485 nm/λ_{em} = 520 nm was 230 ± 30 μM. The phospholipid content was determined by the ferrithiocyanate method according to the protocol from Analytical Control Systems, Inc. (Fishers, IL). Briefly, chloroform, ferrithiocyanate reagent (23.03 g of ferric chloride hexahydrate and 30.4 g of ammonium ferrothiocynate per 1 L of water), and liposomes were mixed at vol/vol ratio of 2:2:0.1, vigorously mixed on a vortex for 60 s, and centrifuged to separate layers. Phospholipid content of the lower chloroform layer was determined by absorbance at 488 nm using DOPC as a standard. The liposomal phospholipid content was 6 ± 1.5 mM. The liposome average size of 93 nm (SD 11) at 26.3° and 105 nm (SD 14) at 35.2° was determined by DELSA 440SX (Coulter-Beckman, Miami, FL). Assembled liposomes retained the same HPTS concentration and ribonuclease activity of HuS after a 1-week storage on ice.

Construction of the pET/Hu$(G_4S)_3$ Vector. The pET29/Hu-tag vector (a derivative of the pET29a(+) bacterial expression vector, Novagen) for expressing recombinant proteins with an N-terminal Hu-peptide was described recently (*3*). To optimize the vector, a DNA fragment encoding an 8-aa linker between the Hu-tag sequence and the multiple cloning site (MCS) was replaced with a DNA fragment encoding a $(G_4S)_3$ peptide

as follows. Two single-stranded DNA fragments (synthesized by GeneLink, Thornwood, NY) were mixed in equimolar concentrations and annealed at room temperature (RT): 5′-pC GGT AGT GGT GGT GGC GGT TCA GGC GGA GGT GGC TC and 5′-pCAT GGA GCC ACC TCC GCC TGA ACC GCC ACC ACC ACT ACC GGT AC. The annealed DNA fragment containing overhangs compatible with *Nco*I and *Kpn*I sites was ligated into *Nco*I−*Kpn*I of the pET29/Hu-tag vector. The *Kpn*I site has been destroyed then by site-directed mutagenesis (Gene-Tailor site-directed mutagenesis kit, Invitrogen) using primers: 5′- GT CAA CAC ATG GAC TCT GGT GGC GGC GGT AGT GGT GG (sense, mutation underlined) and 5′-ACC AGA GTC CAT GTG TTG ACG TTG AAA TTT TTT AGC (antisense). In the resulting pET/Hu$(G_4S)_3$ vector, an N-terminal 15-aa Hu-tag located immediately after the initiator methionine is connected to the MCS region via a $(G_4S)_3$ peptide linker.

Construction and Expression of Hu-Tagged Targeting Proteins. A 121-aa isoform of human vascular endothelial growth factor (VEGF) and human annexin V coding sequences were amplified by PCR using primers introducing *Nco*I sites (underlined) and cloned separately into the *Nco*I site of the pET/Hu$(G_4S)_3$ vector. VEGF was amplified from the pET29/Hu−VEGF plasmid (*3*) with primers 5′-CAC AAG CCA TGG CAC CCA TGG CAG AAG GAG GA (sense) and 5′-AC TAC CCA TGG TCA CCG CCT CGG CTT GTC AC (antisense). Human annexin V was amplified from the pPAP1-1.6 plasmid (kindly provided by Dr. J. Tait, University of Washington School of Medicine, Seattle, WA) with primers 5′-CAC AAG CCA TGG CAC AGG TTC TCA GAG (sense) and AC TAC CCA TGG TTA GTC ATC TTC TCC ACA GAG C (antisense). Clones with ORF correct orientations were selected by PCR using a T7-based sense primer. Both Hu-tagged proteins, Hu−VEGF and Hu−annexin, were expressed in *E. coli* strain BL21(DE3) (Novagen) grown in LB medium (Q-Biogen, Carlsbad, CA). The expression was induced by 1 mM IPTG at the optical density of 0.5−0.7 unit at 600 nm. After induction, the cultures were grown for 2 h at 37 °C with shaking at 300 rpm, then harvested by centrifugation. Hu−VEGF was refolded from inclusion bodies and purified as described (*3*). The yield of Hu−VEGF was 5 mg/L, purity was >95% by SDS−PAGE followed by SimplyBlue Safe Stain (Invitrogen), and dimer content was no less than 95% as estimated by nonreducing SDS−PAGE. Hu−annexin was expressed in a soluble cytoplasmic form and purified as described (*7*) with minor modifications. Briefly, bacterial pellets were resuspended in 50 mM Tris-HCl, 15 mM $CaCl_2$, pH 7.2, in the presence of Protease Inhibitor Cocktail Set II (Calbiochem, La Jolla, CA), then opened by sonication and centrifuged at 15 000*g* for 10 min. The pellet was resuspended in 50 mM Tris-HCl, 30 mM EDTA, pH 7.2, and centrifuged at 17 000*g* for 10 min. The supernatant containing Hu−annexin was dialyzed against 100 volumes of 20 mM Tris-HCl, pH 8.0, for 20 h. Hu−annexin was purified from the dialyzed supernatants by ion-exchange chromatography on HiTrap Q Sepharose Fast Flow (1-mL prepacked columns, Amersham). The yield of Hu−annexin was 15 mg/L, and purity was >95% by SDS−PAGE followed by SimplyBlue Safe Stain (Invitrogen). Both Hu−VEGF and Hu−annexin were stored at −70 °C in small aliquots.

Ribonuclease Activity. Ribonuclease activities of wild-type and mutant BH-RNases and reconstituted ribonuclease activities of assembled complexes were assayed as previously described (*2*, *3*, *5*, *6*). Briefly, varying amounts of RNase or preformed complex were added to a buffer containing 20 mM Tris-HCl, 100 mM NaCl, pH 7.5, 0.1 mg/mL poly C, and incubated for 5 min at RT. Ribonuclease activity was measured by 280-nm absorbance of the reaction mixtures cleared from TCA-precipitated material. One optical unit of TCA-soluble material released from poly C under these conditions was defined as one relative unit of ribonuclease activity.

HuS/Hu-tag Binding Assay. The equilibrium dissociation constant (K_D) values for complexes of HuS mutants and Hu-tagged proteins were determined as previously described (*3*, *5*, *6*). Briefly, HuS(N68C) and HuS(N88C) at final concentrations of 0.1, 0.2, or 0.3 nM were mixed separately with varying amounts of Hu−annexin. Reconstituted ribonuclease activity was measured as described above. Calculations of the K_D values were performed assuming that the initial rate of the hydrolysis is proportional to the concentration of reconstituted ribonuclease. DYNAFIT software was used for the global fitting with numeric iteration and calculation of the K_D values (*8*).

Hu-VEGF Assays. HEK293 human transformed embryonic kidney cells (CRL-1573) were from American Type Culture Collection (Rockville, MD). 293/KDR cells expressing 2.5×10^6 VEGFR-2/cell were described elsewhere (*9*). Cells were grown in DMEM with 10% fetal bovine serum (FBS), 2 mM L-glutamine, and antibiotics at 37 °C, 5% CO_2. HEK293 and 293/KDR cells were plated on 24-well plates, 17.5×10^4 cells/well, shifted to starvation medium (DMEM/0.5% FBS) 6 h later, and incubated in this medium for 16 h at 37 °C, 5% CO_2. For liposome binding experiments, cells were used directly after starvation. For VEGFR-2 autophosphorylation, cells after starvation were shifted to serum-free DMEM with 0.5 mM sodium vanadate for 20 min at 37 °C, then stimulated with Hu−VEGF for 10 min at 37° C, lysed, and analyzed by Western blotting using anti-phosphotyrosine RC20−HRPO conjugate (BD Transduction Labs, San Diego, CA).

Hu−Annexin Erythrocyte Binding Assay. The affinity of Hu−annexin for cell membranes with exposed phosphatidylserine was assayed by its ability to compete with FITC−annexin V (Sigma) for binding to erythrocytes as described (*7*, *10*). Briefly, 10^6 erythrocytes of stabilized human blood (4C Plus Cell Control, Beckman Coulter) were incubated with varying amounts of Hu−annexin in the presence of 5 nM FITC−annexin V in binding buffer (10 mM HEPES, pH 7.4, 136 mM NaCl, 2.5 mM $CaCl_2$) for 15 min at RT. Cells were spun down, resuspended in a binding buffer supplemented with 5 mM EDTA, and spun down again. FITC fluorescence in the supernatants was measured at $\lambda_{ex} = 485$ nm/$\lambda_{em} = 520$ nm.

RESULTS

BH-RNase(G68C) and BH-RNase(N88C) Mutants. On the basis of analysis of a 3D-structure of human RNase I (*11*), we have chosen two residues for introducing unpaired cysteines: N88 and G68. Modeling experiments with RNase I indicated that putative C68 and C88 would be oriented away from HuS domains involved in interactions with Hu-tag (Figure 2A) and therefore expected to be available for chemical cross-linking. Both mutant BH-RNases were expressed in BL21(DE3) *E. coli*, refolded from inclusion bodies, and purified to more than 95% pure proteins with yields of 22 mg/L for BH-RNase(G68C) and 45 mg/L for BH-RNase(N88C). Somewhat surprisingly, both mutants displayed decreased ribonuclease activity (Figure 2B) suggesting either subtle effects of the

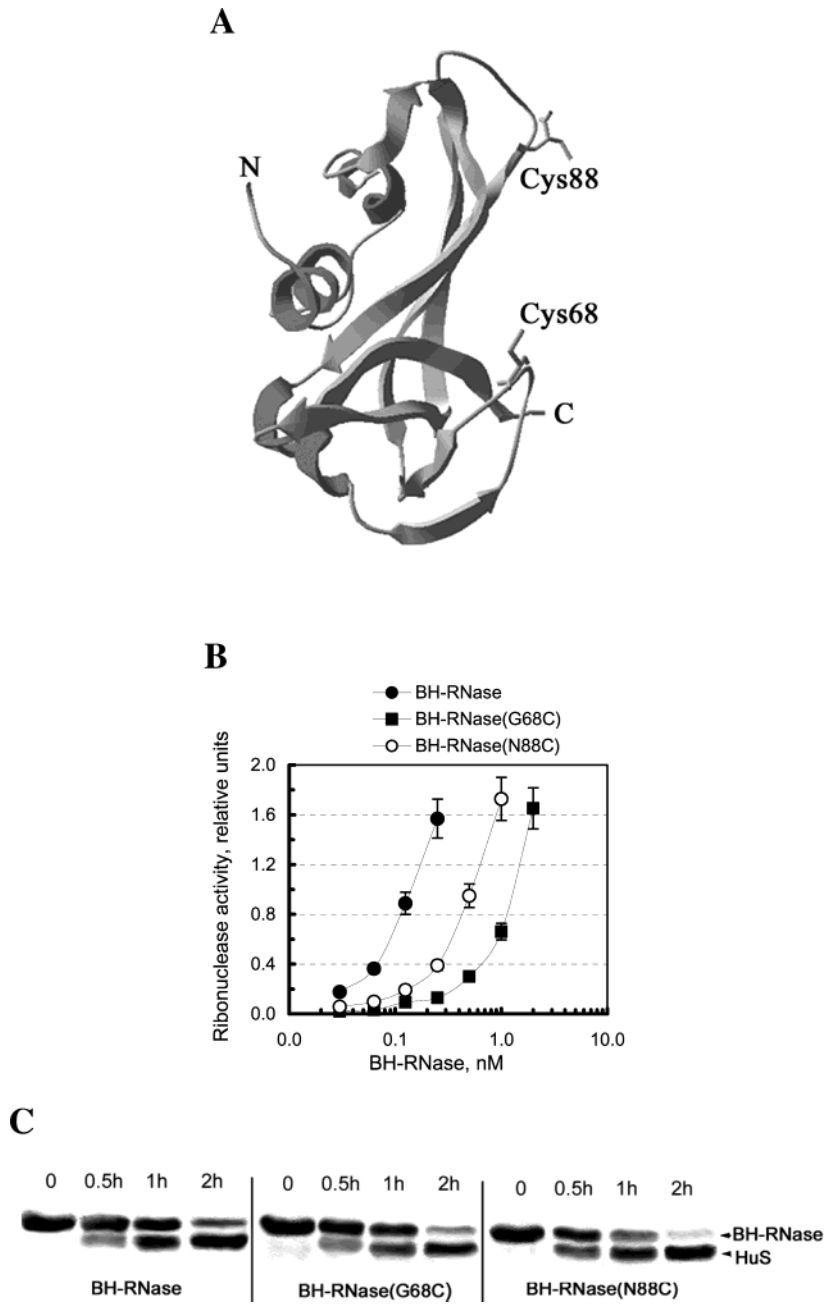

Figure 2. BH-RNase mutants with unpaired cysteines. In panel A, the backbone structure of human RNase I (1E21) is displayed with SWISS-PDB viewer. N- and C-termini and unpaired cysteines in positions 68 and 88 are indicated. Panel B presents the enzymatic activity of BH-RNase mutants. In panel C, wild-type HuS, HuS(G68C), and HuS(N88C) are released from the corresponding BH-RNases by limited digestion with subtilisin at the protease to BH-RNase w/w ratio of 1:50. Digestion reactions were incubated for 0.5, 1, and 2 h at 4 °C and analyzed then by reducing SDS−PAGE on 17.5% gels followed by Simply Blue Safe Stain (Invitrogen).

substitutions on the structure of the active center or the presence of the misfolded mutant BH-RNases in final protein preparations. However, the rates of subtilisin digestion for mutant proteins were comparable to that for wild-type BH-RNase (Figure 2C).

HuS(G68C) and HuS(N88C) Mutants. BH-RNase(G68C) and BH-RNase(N88C) were digested with subtilisin and mutant HuS proteins were purified on a Hu-peptide affinity column as described for wild-type HuS (*5*). To characterize the affinity of purified mutant HuS proteins to Hu-peptide, we used Hu−annexin. A ribbon model of the HuS/Hu−annexin complex is shown in Figure 3A. Reconstituted ribonuclease activity in HuS/Hu−annexin mixtures was measured under conditions of equilibrium between free and bound HuS, and the data were used to calculate the equilibrium dissociation constant (K_D) values for these complexes as described (*3*, *5*, *6*). We found that affinities of HuS(G88C) and HuS(N88C) to Hu−annexin were characterized by the K_D values of 123 ± 26 and 50 ± 6 nM, respectively (Figure 3B,C). Taking into account that BH-RNase(N88C) was recovered as a more active enzyme with a higher yield and its HuS(N88C) fragment displayed higher Hu-tag affinity comparable to that of wild-type HuS (K_D = 29 ± 3 nM (*5*)), further experiments were performed with this mutant.

Availability of C88 for Site-Specific Modification. Since BH-RNase(N88C) mutant was refolded in the presence of reduced/oxidized glutathiones (Red/Ox buffer), we have expected that an unpaired cysteine would be

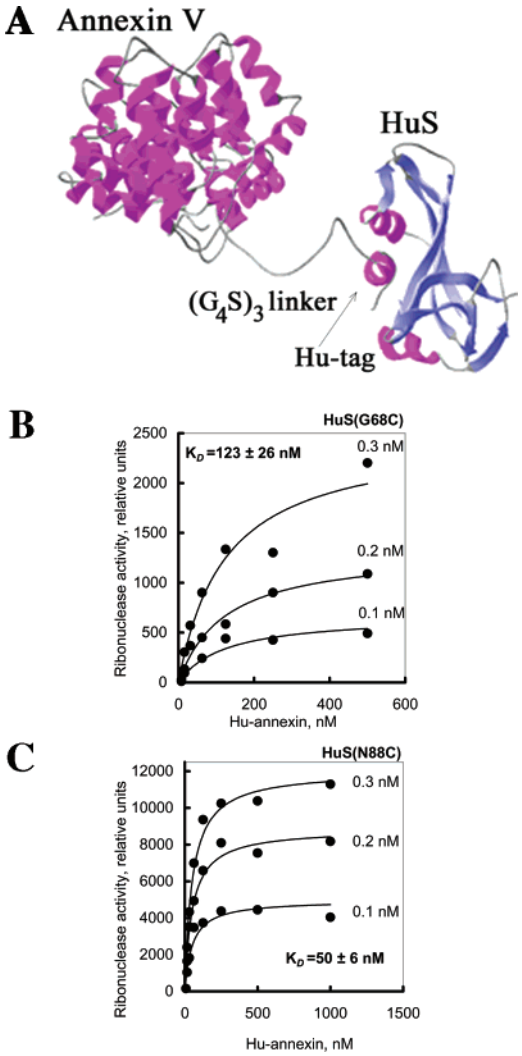

Figure 3. Affinity of HuS mutant proteins for Hu−annexin. Panel A shows the Hu−annexin/HuS complex. The Hu-peptide and $(G_4S)_3$ linker in random orientation were built using SWISS-PDB viewer and linked to the annexin V structure. The Hu−annexin/HuS complex was minimized using the SANDER module of the AMBER software package. Panels B and C show the affinity of HuS/Hu-tag interactions. Fixed amounts (0.1, 0.2, and 0.3 nM) of HuS(G68C) mutant (B) and HuS(N88C) mutant (C) were mixed separately with varying amounts of Hu−annexin. The K_D values for the resulting complexes were calculated as described (*5*, *6*).

involved in a mixed disulfide with glutathione. Mixed disulfides were reported for other recombinant proteins with odd numbers of cysteines refolded in Red/Ox buffers including a mutant bovine S-protein with an engineered cysteine in position 122 (*6*, *12*). Indeed, modification of freshly isolated BH-RNase(N88C) mutant protein with a sulfhydryl-directed reagent *N*-(1-pyrene)-maleimide indicated that only a fraction of unpaired cysteines was accessible for modification, varying from 5% to 35% in different preparations of BH-RNase(N88C). However, after a mild DTT treatment of BH-RNase(N88C) that did not affect RNase activity (1.5-fold molar excess DTT at 4 °C in the presence of 0.5 M NDSB-221 to prevent protein aggregation), the fraction of unpaired cysteines accessible for pyrene modification reached 95−98% indicating release from mixed disulfide (data not shown). To establish the position of a cysteine with a free SH-group, pyrene-modified HuS(N88C) was digested with endoproteinase Arg-C, and the digest was fractionated by RP HPLC. The major pyrene-containing peak (87% of incorporated pyrene) was found to be a single peptide with a mass of 951.43 as provided by electrospray mass spectrometric analysis. This mass corresponded to the theoretical mass of the expected peptide, Leu_{86}-Thr-Cys-(*N*-1-pyrene)-Gly-Ser-Arg_{92} (933.43 kDa) containing C88 modified with pyrene. The remaining pyrene (13%) was incorporated in several minor peaks that were not further analyzed.

Site-Specific Modification of HuS(N88C). To demonstrate utility of HuS(N88C) for developing uniform "payload" modules, we constructed a HuS(N88C)−lipid conjugate and inserted it into HPTS-loaded liposomes. Site-directed modification of C88 with mPEG−DSPE−maleimide included several steps. First, BH-RNase-(N88C) was "deprotected" from mixed disulfides (as described above). Second, it was cleaved with subtilisin, and subtilisin was removed from the reaction mixture by ion-exchange chromatography on an SP-column. Third, digested BH-RNase(N88C) was modified with mPEG−DSPE−maleimide, and the final product was purified on Hu-peptide affinity column (Figure 4A). The latter step removed undigested BH-RNase(N88C) and yielded a mixture of HuS(N88C)−DSPE conjugate and unmodified HuS(N88C). The extent of lipid modification of HuS-(N88C) eluted from affinity column varied from 70% to 85% as judged by RP HPLC analysis (Figure 4B). Two peaks of HuS−DSPE eluted at 23 and 23.6 min were products of conjugation with two forms of mPEG−DSPE−maleimide that are initially present in the reagent and the traces of which, eluted at 25 and 25.6 min, are still detectable in purified HuS−DSPE (Figure 4B). The mixture of HuS(N88C) and HuS(N88C)−DSPE conjugate retained the same ribonuclease activity after several months of storage in liquid nitrogen (data not shown).

For insertion in HPTS-loaded liposomes, the mixture of HuS(N88C)−DSPE conjugate and HuS(N88C) was incubated with liposomes for 16 h at 37 °C, followed by purification on Sepharose 4B and characterization of the size and composition as described in Materials and Methods. The efficiency of HuS(N88C)−DSPE insertion was determined by RP HPLC analysis of purified liposomes (Figure 4C, note that the RP HPLC system is different from the one described in Figure 4B; the peak eluted at 24 min corresponds to liposomal lipids). Based on this analysis, the amount of inserted HuS(N88C)−DSPE varied from 80% to 95% from experiment to experiment.

Hu-Tagged Targeting Proteins. The pET29/Hu-tag vector for bacterial expression of recombinant proteins with an N-terminal Hu-tag has been described recently (*3*). In the new pET$(G_4S)_3$Hu vector constructed for this work, a random 8-aa linker connecting Hu-tag and MCS region of the pET29/Hu-tag vector has been replaced with a standard $(G_4S)_3$ linker designed for fusion of heavy and light chains of monoclonal antibodies (*13*) and widely used since then for construction of single-chain recombinant antibodies (*14*, *15*). Using the pET$(G_4S)_3$Hu vector, we have expressed two targeting proteins, Hu−VEGF and Hu−annexin.

Functional activity of Hu−annexin was determined as its ability to compete with FITC−annexin for binding to phosphatidylserine-displaying erythrocytes of stabilized human blood (*7*). In this assay, annexin is bound to erythrocytes in the presence of Ca^{2+} and released in the presence of EDTA. We found that Hu−annexin displaced FITC−annexin in a dose-dependent manner with IC_{50} of 11 ± 3 nM (Figure 5A). Since correct size recombinant

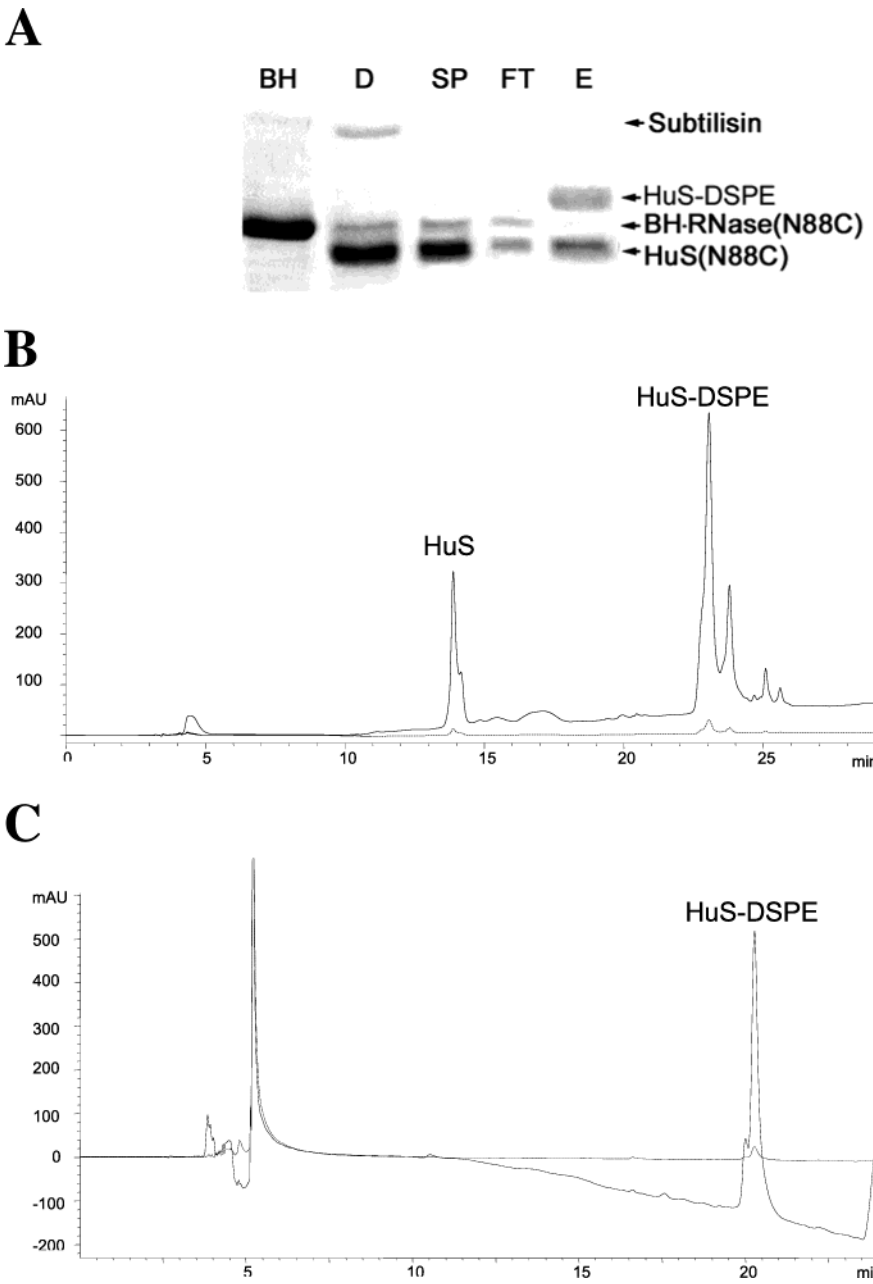

Figure 4. HuS88C−DPDE cross-linking and insertion into liposomes. Panel A shows SDS−PAGE analysis of HuS(N88C)−DSPE conjugate synthesis and purification: lane BH, BH-RNase(N88C); lane D, digestion of BH-RNase(N88C) with subtilisin; lane SP, SP-column purification; lane FT, affinity Hu-column flow-through; lane E, elution from affinity Hu-column. Samples were analyzed by reducing SDS−PAGE on 17.5% gels followed by Simply Blue Safe Stain (Invitrogen). In panel B, HuS(N88C)−DSPE was affinity purified and analyzed by RP HPLC (50 mM thriethylamine phosphate, pH 2.8, 20% 2-propanol with a linear gradient of acetonitrile 0−70% over 30 min). The yield of modified product was calculated as a ratio of integral peak intensities for HuS(N88C)−DSPE conjugate and unmodified HuS(N88C); in this case, modification is 77%. In panel C, the HuS(N88C)−DSPE conjugate was inserted in liposomes (16 h at 37 °C) and then analyzed by RP HPLC (50 mM thriethylamine phosphate, pH 2.8, and 20% tetrahydrofuran with a linear gradient of acetonitrile 0−70% over 25 min).

annexin V displayed a similar activity in this assay (IC_{50} of 9 ± 4 nM, (*7*)), we concluded that fusion of the Hu-tag did not disturb annexin V functional activity.

Functional activity of Hu−VEGF was tested in a VEGFR-2 autophosphorylation assay (Figure 5B). Hu−VEGF induced VEGFR-2 tyrosine autophosphorylation in 293/KDR cells, which was detectable at 0.04 nM Hu−VEGF and reached plateau at 0.4 nM (Figure 5B). Since similar activities were reported for the previous version of Hu−VEGF with a random 8-aa linker and also for recombinant human $VEGF_{165}$ (*3*), we concluded that the extension of the linker from 8-aa to 15-aa did not have detrimental effects on VEGF functional activity.

Targeted Delivery of HuS−Liposomes. Targeting proteins were mixed with HPTS-containing HuS−liposome at equimolar Hu-tagged protein to HuS ratio, and the HuS/Hu-tag association was detected by reconstituted ribonuclease activity. We found that dose-dependencies of ribonuclease activity of complexes with liposome-bound HuS were similar to that obtained with free HuS (Figure 6A). Targeting of HuS−Lip/Hu−annexin was tested in an erythrocyte binding assay. HuS−liposomes were used as a control for a nonspecific binding. We found that Hu−annexin/HuS−liposome complexes bound to erythrocytes in a dose-dependent manner, and the levels of binding

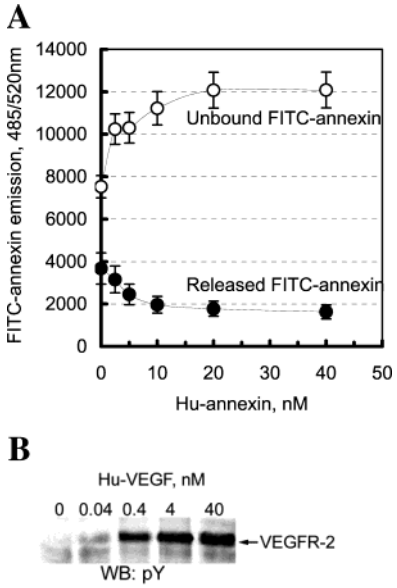

Figure 5. Hu-tagged targeting proteins are functionally active. In panel A, Hu−annexin competes with FITC−annexin for binding to erythrocytes with exposed phosphatidylserine. Unbound FITC−annexin was found in the supernatants after binding with erythrocytes; released FITC−annexin was found in the supernatants after resuspension of erythrocytes in EDTA-containing buffer. In panel B, Hu−VEGF activates VEGFR-2 in 293/KDR cells.

were significantly higher amounts than that for untargeted HuS−liposomes (Figure 6B).

Targeting of HuS−Lip/Hu−VEGF was tested in a binding assay with 293/KDR cells expressing 2.5×10^6 VEGFR-2/cell (9). HuS−liposomes were used as a control for a nonspecific binding. In addition, HEK293 cells lacking VEGFR-2 were used as a control for non-VEGFR-2-mediated binding. We found that 293/KDR cells internalized VEGF-driven HuS−liposomes significantly better than nontargeted HuS−liposomes (Figure 6C). In contrast, both targeted and nontargeted liposomes were internalized to the same extent by HEK293 cells lacking VEGFR-2 (Figure 6C).

DISCUSSION

To eliminate random chemical modification of targeting proteins currently used for targeted delivery of therapeutics and diagnostics, we have recently proposed to link a cargo to a standardized adapter protein that binds noncovalently to a docking tag engineered into a targeting protein (Figure 1). This approach however still yielded heterogeneous targeted drug delivery complexes because of a random cross-linking of a cargo to the adapter protein. Here we report development of a novel HuS(N88C) adapter protein for assembly of targeting drug delivery complexes (Figure 1). This mutant carries an unpaired cysteine in position 88 available for site-directed conjugations of drugs or drug carriers.

We have recently developed a high-yield system for production of HuS protein by subtilisin digestion of a chimeric recombinant BH-RNase containing an appropriate subtilisin cleavage site (*5*). BH-RNase is easily refolded into a functionally active conformation and yielded highly active HuS after subtilisin digestion. Therefore, to develop HuS mutants with unpaired cysteines, we mutated BH-RNase and then recovered HuS mutants by subtilisin digestion of the corresponding BH-RNases. The positions for the G68C and N88C substitutions have been chosen on the basis of 3-D structure of human RNase I (*11*) with the goal to minimize possible interference of cross-linked constructs with tag/adapter interactions. We report here that both mutant HuS proteins are readily recovered from the corresponding mutant BH-RNases by subtilisin digestion followed by affinity purification. We found that HuS(N88C) is a better candidate for further development because of its higher yield and higher affinity to Hu-tag, which is close to that of wild-type HuS (Figure 3 B,C (*5*)). A point mutation in position 88 of bovine RNase A was shown to decrease RNase affinity to ribonuclease inhibitor (RI) and enhances cytotoxic activity of RNase A (*16*). However, mutations in positions 88, 89, or 90 of highly homologous RNase I had little, if any, effect on cytotoxicity of this protein (*17*). Nevertheless, one could expect that cross-linking of bulky compounds to C88 still could decrease affinity of the reconstituted RNase to RI providing the assembled complexes with intrinsic cytotoxicity, which would be an additional benefit in a case of delivery of cytotoxic drugs.

Using maleimide chemistry, we cross-linked a PEGylated lipid to HuS(N88C). HuS−lipid conjugate was inserted into preformed unilamellar liposomes yielding 20−30 adapter proteins per liposome, which is consistent with previously published data on immunoliposome construction (*18*). HuS−liposomes readily bind Hu-tagged proteins as judged by reconstitution of RNase activity upon HuS/Hu-tag interaction. Furthermore, liposomes linked to HuS via C88 did not affect adapter/tag interactions, since complexes reconstituted with both liposomal and free HuS protein displayed similar ribonuclease activities. No significant interference with adapter/tag interactions was also observed in our preliminary experiments with various bulky constructs, such as magnetic beads (Dynal Biotech Corp., Lake Success, NY) or Dexferrum magnetic particles, (American Regent Lab., Shirley, NY) linked to HuS via C88.

Assembled drug delivery complexes might be developed for therapeutic applications only if their cargo does not interfere with targeting protein/receptor interaction. We report here that two different targeting proteins, Hu−annexin V and Hu−VEGF, significantly enhance HuS−liposome binding to the corresponding cells. Thus, liposomes do not interfere with binding of these targeting proteins to their cellular targets. Since annexin V and VEGF are vastly different proteins with even more different targets, we expect that HuS−liposomes developed in this work can be used as a standardized payload module for delivery by various targeting proteins. Although assembly of targeting complexes described in this work requires production of a modified adapter protein, this approach provides significant advantages over traditional drug loading via direct conjugation to targeting proteins. First, the same modified adapter would be suitable for assembly with different targeting proteins. Second, since the site-specifically modified adapter retains the ability to bind targeting proteins, we expect that various drugs or drug carriers can be cross-linked to C88 via standardized chemistries. We therefore expect that the benefits associated with the elimination of both the damage to the targeting proteins and the heterogeneity of the final products would stimulate acceptance of assembled complexes for targeted drug delivery. Experiments are in progress to establish whether selectivity provided by assembled targeting complexes is sufficient for therapeutic and diagnostic applications.

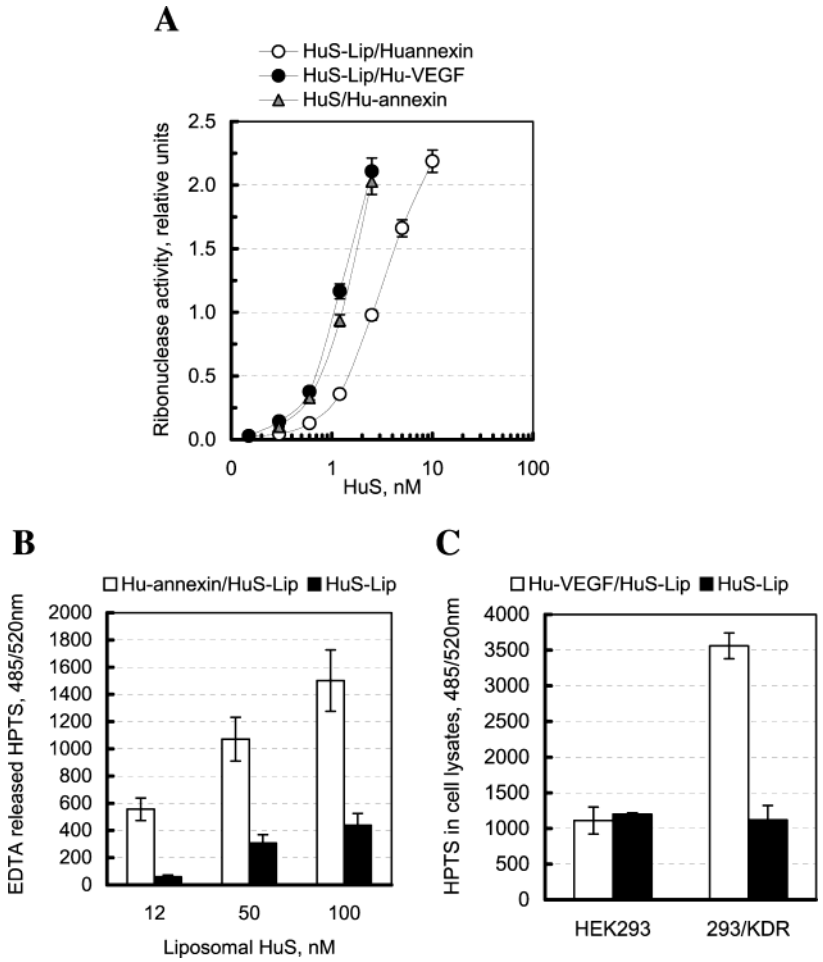

Figure 6. Targeted delivery of HiS−liposomes. Hu-tagged targeting proteins were mixed separately with HuS−liposomes at the liposomal HuS to Hu-tagged protein molar ratio of 1:1. For the liposome alone control (HuS−Lip), equal volumes of protein storage buffer were added to liposomes. All complexes were incubated on ice for 15 min and then added to cells. HPTS fluorescence was measured at λ_{ex} = 485 nm/λ_{em} = 520 nm. Liposome delivery experiments were done in duplicate and repeated twice. In panel A, Hu−annexin and Hu−VEGF bind HuS−liposomes with restoration of ribonuclease activity. In panel B, Hu−annexin-driven liposomes were added to erythrocytes in binding buffer at indicated liposomal HuS concentrations, incubated for 15 min at RT, and then spun down. The pellets were washed twice with binding buffer prior to resuspension in EDTA-containing buffer, then spun down again. HPTS fluorescence was measured in the supernatants. In panel C, Hu−VEGF-driven liposomes were added to starved HEK/293 and 293/KDR cells to final concentrations of 60 nM complex HuS/dimer VEGF. Cells were incubated 45 min at 4 °C and then moved to 37 °C to allow internalization of complexes. After 45 min at 37 °C, cells were washed twice with PBS and once with PBS containing 0.4 M NaCl and lysed in PBS with 1% NP-40. HPTS fluorescence was measured in the clarified cell lysates.

ACKNOWLEDGMENT

This work was supported by Grants DAMD17-03-C-0011 from Department of Defense and DE-FG02-02ER83520 from Department of Energy.

LITERATURE CITED

(1) Dubowchik, G. M, and Walker, M. A. (1999) Receptor-mediated and enzyme-dependent targeting of cytotoxic anti-cancer drugs. *Pharmacol. Ther. 83*, 67−123.

(2) Backer, M. V., Aloise, R., Przekop, K., Stoletov, K., and Backer, J. M. (2002) Molecular vehicles for targeted drug delivery. *Bioconjugate Chem. 13*, 462−467.

(3) Backer, M. V., Gaynutdinov, T. I., Gorshkova, I. I., Crouch, R. J., Hu, T., Aloise, R., Arab, M., Przekop, K., and Backer, J. B. (2003) Humanized docking system for assembly of targeting drug delivery complexes. *J. Controlled Release, 89*, 499−511.

(4) Blankenberg, F. G., Mandl, S., Cao, Y.-A., O'Connell-Rodwell, C., Contag, C., Mari, C., Gaynutdinov, T. I., Vanderheyden, J.-L., Backer, M. V., and Backer, J. M. (2004) Tumor imaging using a standardized radiolabeled adapter protein docked to vascular endothelial growth factor (VEGF). *J. Nucl. Med.*, in press.

(5) Gaynutdinov, T. I., Myshkin, E., Backer, J. M., and Backer, M. V. (2003) Chimeric ribonuclease as a source of human adapter protein for targeted drug delivery. *Prot. Eng. 16*, 771−775.

(6) Backer, M. V., Gaynutdinov, T. I., Aloise, R., Przekop, K., and Backer, J. (2002) Engineering S-protein fragments of bovine ribonuclease A for targeted drug delivery. *Protein Expression Purif. 26*, 455−461.

(7) Tait, J. F., Smith, C., and Gibson, D. F. (2002) Development of annexin V mutants suitable for labeling with Tc(I)-carbonyl complex. *Bioconjugate Chem. 13*, 1119−1123.

(8) Kuzmic, P. (1996) Program DYNAFIT for the analysis of enzyme kinetic data: Application to HIV proteinase. *Anal. Biochem. 237*, 260−273.

(9) Backer, M. V., and Backer, J. M. (2001) Functionally active VEGF fusion proteins. *Protein. Expression Purif. 23*, 1−7.

(10) Tait, J. F., Engelhardt, S., Smith, C., and Fujikawa, K. (1995) Pourokinase-annexin V chimeras. Construction, expression, and characterization of recombinant proteins. *J. Biol. Chem. 270*, 21594−21599.

(11) Pous, J., Mallorquí-Fernández, G., Peracaula, R., Terzyan, S. S., Futami, J., Tada, H., Yamada, H., Seno, M., de Llorens,

R., Gomis-Rüth, F. X., and Coll, M. (2001) Three-dimensional structure of human RNase 1 delta N7 at 1.9 Å resolution. *Acta Crystallogr., Sect. D.: Biol. Crystallogr. 57*, 498−505.

(12) Proba, K., Honneger, A., and Pluckthun, A. (1997) A natural antibody missing a cysteine in Vh: consequences in thermodynamic stability and folding. *J. Mol. Biol. 265*, 161−172.

(13) Huston, J. S., Levinson, D., Mudgett-Hunter, M., Tai, M. S., Novotný, J., Margolies, M. N., Ridge, R. J., Bruccoleri, R. E., Haber, E., and Crea, R. (1988) Protein engineering of antibody binding sites: recovery of specific activity in an anti-digoxin single-chain Fv analogue produced in *Escherichia coli*. *Proc. Natl. Acad. Sci. U.S.A. 85*, 5879−5883.

(14) Shan, D., Press, O. W., Tsu, T. T., Hayden, M. S., and Ledbetter, J. A. (1999) Characterization of scFv-Ig constructs generated from the anti-CD20 mAb 1F5 using linker peptides of varying lengths. *J. Immunol. 162*, 6589−6595.

(15) Feng, J., Xie, Z., Guo, N., and She, B. (2003) Design and assembly of anti-CD16 ScFv antibody with two different linker peptides. *J. Immunol. Methods 282*, 33−43.

(16) Leland, P. A., L. Schultz, W., Kim, B.-M., and Raines, R. T. (1998) Ribonuclease A variants with potent cytotoxic activity. *Proc. Natl. Acad. Sci. U.S.A. 95*, 10407−10412.

(17) Gaur, D., Swaminathan, S., and Batra, J. K. (2001) Interaction of Human Pancreatic Ribonuclease with Human Ribonuclease Inhibitor. *J. Biol. Chem. 276*, 24978−24984.

(18) Spragg, D. D., Alford, D. R., Greferath, R., Larsen, C. E., Lee, K.-D., Gurtner, G. C., Cybulsky, M. I., Tosi P. F., Nicolau, C., and Gimbrone, M. A., Jr. (1997) Immunotargeting of liposomes to activated vascular endothelial cells: A strategy for site-selective delivery in the cardiovascular system. *Proc. Natl. Acad. Sci. U.S.A. 94*, 8795−8800.

BC0499477